ORIGINAL RESEARCH

P300/CBP Regulates HIF-1–Dependent Sympathetic Activation and Hypertension by Intermittent Hypoxia

Ning Wang, Xiaoyu Su, David Sams, Nanduri R. Prabhakar, and Jayasri Nanduri

Institute for Integrative Physiology and Center for Systems Biology of O_2 Sensing, The University of Chicago, Chicago, Illinois

ORCID ID: 0000-0003-3984-7447 (J.N.).

Abstract

Obstructive sleep apnea (OSA), a widespread breathing disorder, leads to intermittent hypoxia (IH). Patients with OSA and IH-treated rodents exhibit heightened sympathetic nerve activity and hypertension. Previous studies reported transcriptional activation of nicotinamide adenine dinucleotide phosphate (NADPH) oxidases (Nox) by HIF-1 (hypoxia-inducible factor-1) contribute to autonomic dysfunction in IH-treated rodents. Lysine acetylation, regulated by KATs (lysine acetyltransferases) and KDACs (lysine deacetylases), activates gene transcription and plays an important role in several physiological and pathological processes. This study tested the hypothesis that acetylation of HIF-1α by p300/CBP (CREB-binding protein) (KAT) activates Nox transcription, leading to sympathetic activation and hypertension. Experiments were performed on pheochromocytoma-12 cells and rats treated with IH. IH increased KAT activity, p300/CBP protein, HIF-1α lysine acetylation, HIF-1 transcription, and HIF-1 binding to the *Nox4* gene promoter in pheochromocytoma-12 cells, and these responses were blocked by CTK7A, a selective p300/CBP inhibitor. Plasma norepinephrine (index of sympathetic activation) and blood pressures were elevated in IH-treated rats. These responses were associated with elevated p300/CBP protein, HIF-1α stabilization, transcriptional activation of *Nox2* and *Nox4* genes, and reactive oxygen species, and all these responses were absent in CTK7A-treated IH rats. These findings suggest lysine acetylation of HIF-1α by p300/CBP is an important contributor to sympathetic excitation and hypertension by IH.

Keywords: histone acetylases; hypoxia inducible factor-1; intermittent hypoxia; p300/CBP; obstructive sleep apnea

Obstructive sleep apnea (OSA) is a widespread breathing disorder characterized by periodic cessation of breathing during sleep, affecting several million people in the United States alone (1, 2). Intermittent hypoxia (IH) is a hallmark manifestation of OSA and a major factor contributing to OSA-related cardiovascular pathology. Rodents treated with IH patterned after blood O_2 profiles in OSA exhibit sympathetic nervous system activation and hypertension, a phenotype reported in patients with OSA (3–6). Experimental studies identified that HIF-1 (hypoxia inducible factor-1)-dependent activation of nicotinamide adenine dinucleotide phosphate (NADPH) oxidases (Nox) and the resulting increase in oxidative stress is an important molecular mechanism underlying IH-evoked sympathetic activation (7, 8). Mice with partial deficiency of HIF-1α, the O_2-regulated subunit of the HIF-1 complex, exhibit remarkable absence of IH-evoked sympathetic activation and hypertension (9).

Stabilization of HIF-1α protein is an essential prerequisite for initiating HIF-1–dependent transcription. HIF-1α stabilization by IH involves, in part, hydroxylation of prolyl residues (7). In addition to hydroxylation, lysine acetylation is another important post-translational modification contributing to HIF-1α stabilization (10, 11). Lysine acetylation is mediated by lysine acetyltransferases (KATs). P300 and CBP (CREB-binding protein) are widely studied members of the KAT family and share considerable sequence homology. Mice harboring a homozygous deletion of either p300 ($p300^{-/-}$) or CBP ($CBP^{-/-}$) or a double heterozygous ($p300^{+/-}/CBP^{+/-}$) deletion show embryonic lethal phenotypes (12, 13).

Several lines of evidence suggest that p300/CBP is a critical component of the HIF-1 transcriptional complex (14–17). HIF-1α has multiple acetylation sites, and downstream effects of HIF-1α acetylation vary depending on the modified lysine

(Received in original form December 15, 2022; accepted in final form October 23, 2023)

Supported by National Institutes of Health grant P01-HL144454.

Author Contributions: J.N. conceived and designed the experiments. N.W., X.S., and D.S. performed experiments and analyzed the data. J.N wrote and N.R.P edited the manuscript.

Correspondence and requests for reprints should be addressed to Jayasri Nanduri, Ph.D., Institute for Integrative Physiology and The Center for Systems Biology of O_2 Sensing, University of Chicago, 5841 South Maryland Avenue, Chicago, IL 60637. E-mail: jnanduri@uchicago.edu.

This article has a related editorial.

This article has a data supplement, which is accessible from this issue's table of contents at www.atsjournals.org.

Am J Respir Cell Mol Biol Vol 70, Iss 2, pp 110–118, February 2024

Originally Published in Press as DOI: 10.1165/rcmb.2022-0481OC on October 24, 2023
Internet address: www.atsjournals.org

Clinical Relevance

To the best of our knowledge, results of this manuscript provide a hitherto uncharacterized role for p300/CBP as regulators of HIF-1 (hypoxia-inducible factor-1)-dependent transcriptional activation causing hypertension under the setting of intermittent hypoxia (IH). Given the broad physiological importance of p300/CBP and HIF-1 in health and disease, our results are of considerable biological and therapeutic significance for preventing cardiovascular morbidities caused by IH such as that occurring in obstructive sleep apnea patients.

residue (18, 19). However, little information is available on the role of p300/CBP on HIF-1α lysine acetylation and transcription by IH. In the present study, we tested the hypothesis that lysine acetylation by p300/CBP stabilizes HIF-1α protein during IH and increases HIF-1 transcription of the genes encoding NADPH oxidase (e.g., *Nox-4*), thereby contributing to sympathetic activation and hypertension by IH. This hypothesis was tested first in pheochromocytoma (PC12) cells and assessed the significance of HIF-1α acetylation on IH-evoked sympathetic activation and blood pressure (BP) in rats.

Methods

Experimental protocols were approved by the Institutional Animal Care and Use Committee of the University of Chicago (approved protocol #71811). Experiments were performed on age- and sex-matched 4-month-old Sprague Dawley rats. Detailed description of methods, antibodies, primer information, and statistical analysis are provided in the data supplement.

Exposure of Rats and PC12 Cells to IH

Rats were exposed to alternating cycles of hypoxia between 9:00 A.M. and 5:00 P.M. for 10 days, as described previously (9). PC12 cells (20) were exposed to IH, as described (21). In the experiments involving drug treatment, cells were preincubated for 30 minutes before and during IH exposure.

BP and Plasma Norepinephrine Measurement

BP was measured in rats by the tail-cuff method, using a noninvasive BP system (IITC Life Science Inc.). Plasma norepinephrine concentrations were determined by high-pressure liquid chromatography (9).

KAT Activity and Malondialdehyde Levels

KAT activity was measured in nuclear lysates using the colorimetric Epigenase KAT activity kit (Epigentek, Farmington, NY), as per manufacturer's instruction. Malondialdehyde (MDA) concentrations were measured in the cell lysates using the TBARS assay kit (Cayman Chemical Company), as described (9).

Immunoblot Assays

PC12 cell and rat adrenal medulla (AM) cell extracts were fractionated by polyacrylamide-SDS gel electrophoresis. Immunoblots were probed with the primary antibodies (*see* Table E1 in the data supplement) followed by corresponding horseradish peroxidase-conjugated secondary antibody and detected using the Clarity Western ECL substrate kit (Bio-Rad). Immunoblots were quantified using Image studio software by Odyssey Fc imaging system (LI-COR). Raw pixel data for each protein is normalized to loading control (tubulin) and visualized as scaled cluster heatmaps in R studio (v4.2.2) using heatmaply. In addition, data are also expressed as fold change relative to mean vehicle-treated control under normoxia.

qRT-PCR

qRT-PCR was performed using iScript cDNA synthesis kit and SsoFast EvaGreen (Bio-Rad) as a fluorogenic binding dye. Housekeeping genes 18S RNA and β-actin were included as controls for quantitation. Changes in target mRNA expression were calculated based on the Δ(ΔCt) method, as described previously (22). Primer sequences are listed in Table E2.

HIF-1 Reporter Gene Assay

Cells were cotransfected with reporter plasmid p2.1, which contains a 68-bp hypoxia response element (HRE) from the human *EPO1* gene (23), and *Renilla* luciferase control reporter vector (pRL). The Bright-Glo Luciferase Assay System (Promega) was used to measure luciferase activity in nuclear lysates.

Chromatin Immunoprecipitation Assay

Chipped DNA and input DNA were analyzed by qPCR (Primer sequences listed in Table E2), as described previously (24). The percent input method was used to represent the data, which was calculated by the equation $2^{((Ct(IN)-\log2(DF))-Ct(IP))} \times 100$. DF, dilution factor, is the ratio of sample volume lysate used for immunoprecipitate (IP) and input (IN) processing.

Statistical Analysis

Data are expressed as mean ± SEM from three to six independent cell culture experiments and six to eight rats per group per experiment. Data were analyzed using one-way or two-way ANOVA followed by a *post hoc* Tukey honestly significant difference (HSD) test as appropriate (Table E3).

Results

IH Increases KAT Activity and p300/CBP Protein Expression in PC12 Cells

The effect of IH on p300/CBP was studied in PC12 cells because they respond to IH with robust activation of HIF-1 (7). KAT enzyme activity was determined in PC12 cells treated with 60 cycles of IH (IH_{60}) or room air (N: controls). IH_{60} was chosen because it activates HIF-1 transcription (14). IH increased KAT enzyme activity (Figure 1A). Trichostatin A (TSA), an inhibitor of KDACs (25, 26), also increased KAT activity compared with vehicle-treated controls, similar to IH (Figure 1A). We determined whether augmented KAT activity is associated with increased KAT protein. Both IH and TSA increased p300/CBP protein, which belongs to the TIP 60 family of KATs (Figures 1B–1D). In contrast, PCAF and GCN5 (GNAT family of KATs) decreased with IH (Figures 1B and 1C) but not with TSA (Figures 1D and 1E). These results demonstrate IH selectively increases p300/CBP protein in PC12 cells.

We then assessed whether p300/CBP contributes to increased KAT activity by IH. Cells were treated with CTK7A, a curcumin-derived water-soluble, cell-permeable inhibitor of p300/CBP (27). The effect of different concentrations of CTK7A on p300/CBP protein in the nuclear fractions was analyzed; ⩾50 μM CTK7A decreased cell viability under normoxia as measured by Trypan blue exclusion assay (data not shown). On the other hand, 10 μM and

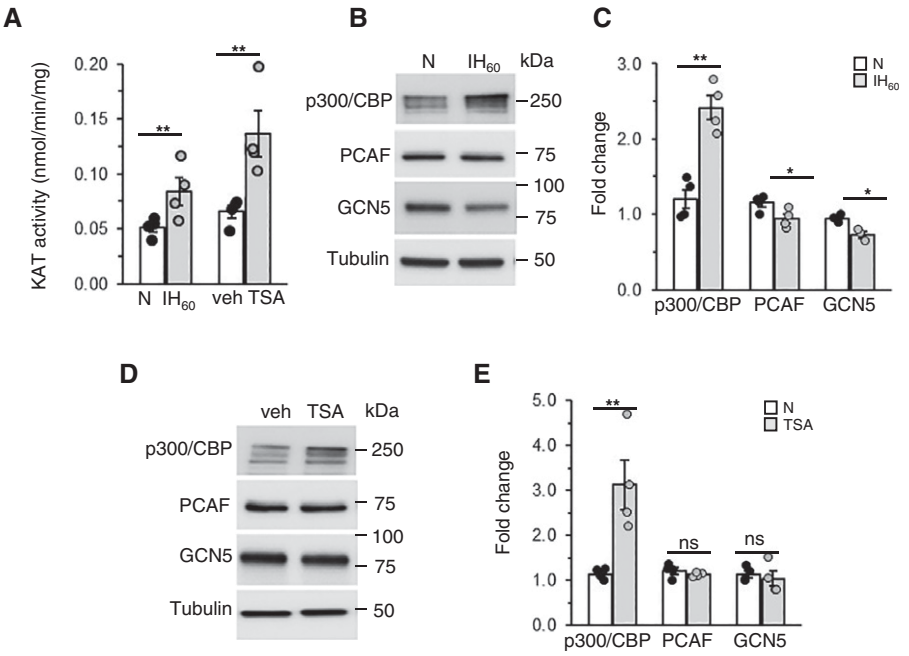

Figure 1. Intermittent hypoxia (IH) increases KAT (lysine acetyltransferase) activity and KAT proteins p300/CBP (CREB-binding protein) in PC12 (pheochromocytoma) cells treated with 60 cycles of IH (IH_{60}). (*A*) KAT activity in nuclear lysates from PC12 cells treated with either normoxia (N) or IH_{60} or treated with 50 nM Trichostatin A (TSA), a KDAC (lysine deacetylase) inhibitor, for 7 hours in room air. Data presented are mean ± SEM; $n = 4$ individual experiments. (*B*) Representative immunoblot showing p300/CBP, PCAF, and GCN5 protein expression with tubulin as a loading control in lysates from room air– and IH-exposed cells. (*C*) Densitometric analysis of immunoblots. (*D*) Representative immunoblot showing p300/CBP, PCAF, and GCN5 protein expression with tubulin as a loading control in lysates from room air treated with vehicle (veh)- or TSA (50 nM)-treated cells. (*E*) Densitometric analysis of immunoblots. Image Studio software by Odyssey Fc imaging system was used for immunoblot quantification. Raw pixel values are normalized to tubulin loading control and expressed as fold change relative to a normoxic control. *P* values (**$P \leq 0.01$, *$P < 0.05$, and ns = not significant) compared with normoxia or vehicle-treated controls as determined by *post hoc* Tukey honestly significant difference (HSD) test. Data from four individual experiments. ns = not significant; veh = vehicle.

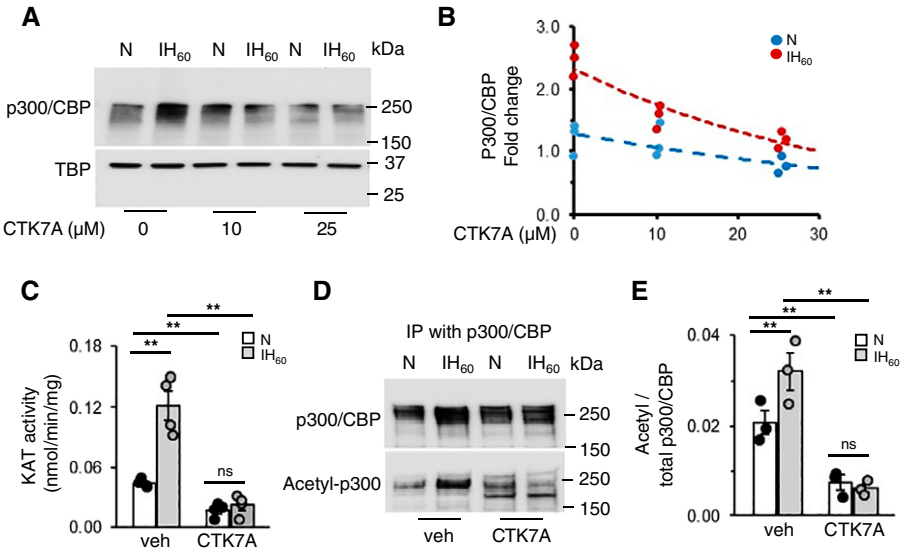

Figure 2. P300/CBP is autoacetylated and stabilized in IH-treated PC12 cells. (*A*) Representative immunoblot showing p300/CBP and TBP (TATA-binding protein) as loading control in nuclear lysates of PC12 cells exposed to normoxia (N) or IH_{60} treated with different concentrations of CTK7A (inhibitor of p300/CBP) run on the same gel. (*B*) Densitometric analysis of the immunoblots. (*C*) KAT activity in IH_{60}- or normoxia-exposed cells treated with veh or CTK7A. (*D*) Nuclear cell lysates from IH_{60}- or normoxia-exposed PC12 cells treated with and without CTK7A were immunoprecipitated (IP) with anti-p300/CBP antibody. Representative immunoblot showing immunoprecipitate replicates run on the same gel and probed with anti-p300/CBP and anti–acetyl-lysine antibodies. (*E*) Densitometric analysis of the immune blots showing ratio of acetyl p300/CBP to total p300/CBP. *P* values (**$P \leq 0.01$) between different groups as determined by *post hoc* Tukey HSD test. Data are mean ± SEM from three to four experiments.

25 μM CTK7A inhibited the increased p300/CBP protein by IH in a concentration-dependent manner (Figures 2A and 2B). Because higher concentrations were toxic to cells and may have nonselective effects (27), 25 μM of CTK7A was used in all subsequent experiments; 25 μM CTK7A decreased KAT enzyme activity in cells exposed to either normoxia or IH (Figure 2C). These results indicated that p300/CBP contributes to increased KAT activity by IH.

Autoacetylation Stabilizes p300/CBP Protein in Response to IH

We next determined how IH increase p300/CBP protein. Autoacetylation-mediated stabilization of p300/CBP enhances its acetyltransferase activity (28). We assessed the autoacetylation status of p300/CBP in response to IH by coimmunoprecipitation assays, because pan-acetylated lysine antibody was not sensitive enough to detect p300/CBP acetylation in total cell lysates. IH-increased total p300/CBP protein was accompanied by a parallel increase in acetylated p300/CBP, with an increase in the ratio of acetyl p300/CBP to total p300/CBP. These effects were absent in IH cells treated with CTK7A (Figures 2D and 2E). However, CTK7A-treated cell lysates showed bands at lower molecular weights in both IH and in normoxia, likely representing degraded products (Figure 2D). These results suggest that IH increases auto-acetylation of p300/CBP protein.

p300/CBP Protein Is Required for HIF-1α Acetylation and Stabilization by IH

We then investigated whether p300/CBP contributes to HIF-1α acetylation and stabilization by IH. HIF-1α abundance increased in nuclear lysates of IH-treated cells, which was reduced with 25 μM CTK7A (Figures 3A and 3B). These results indicated increased HIF-1α protein might involve lysine acetylation by p300/CBP. However, demonstrating acetylation of endogenous HIF-1α in native PC12 cells proved technically challenging because of low abundance of acetylated HIF-1α. To circumvent this limitation, PC12 cells were transfected with a FLAG-tagged HIF-1α–expressing plasmid or a control plasmid (p3X FLAG-CMV) and exposed to IH. Cells with ectopic expression showed higher HIF-1α protein under normoxia and in response to IH than cells expressing control plasmid (Figure 3C). Treating cells with CTK7A blocked HIF-1α levels in both normoxia and IH (Figure 3C).

To demonstrate lysine acetylation, coimmunoprecipitation assay was performed in nuclear lysates of HIF-1α–overexpressing cells with anti-lysine acetylated antibody. IH increased lysine-acetylated HIF-1α and total HIF-1α, and these effects were blocked by CTK7A (Figures 3D and 3E). We next analyzed if p300/CBP binds directly with HIF-1α in a complex to acetylate and stabilize HIF-1α in response to IH. Coimmunoprecipitation experiments showed binding of p300/CBP to HIF-1α, which was blocked with CTK7A (Figures 3D and 3F). Similar results were obtained when endogenous HIF-1α was coimmunoprecipitated with p300/CBP (Figure E1). These findings demonstrate that p300/CBP increases HIF-1α acetylation by physically interacting with HIF-1α and suggest lysine acetylation contributes in part to HIF-1α stabilization by IH.

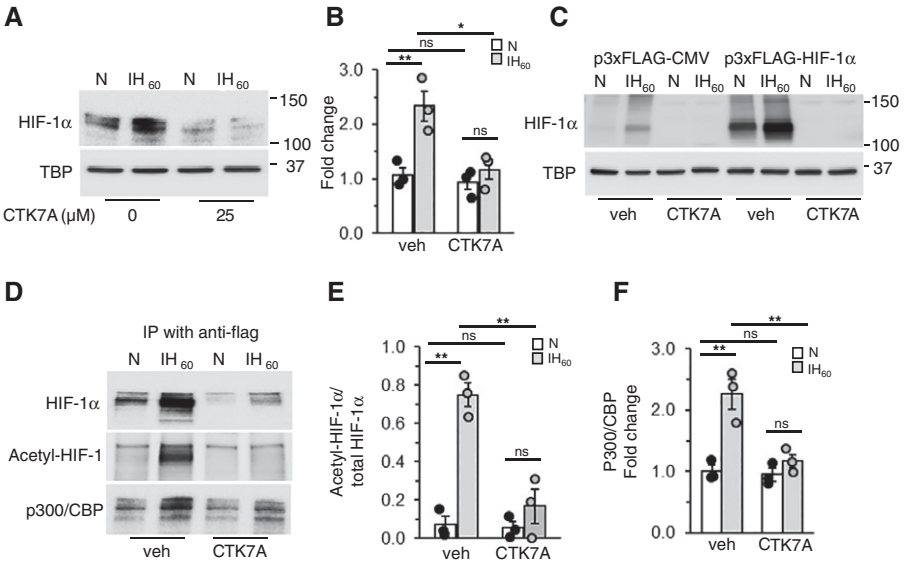

Figure 3. p300/CBP acetylates and stabilizes HIF-1α in PC12 cells treated with IH. (*A*) Representative immunoblot showing HIF-1α expression with TBP as loading control in IH_{60}- or normoxia-exposed PC12 cells treated with either vehicle or CTK7A (25 μM) run on the same gel. (*B*) Densitometric analysis of the HIF-1α immunoblots. (*C*) HIF-1α protein expression in nuclear lysates of PC12 cells transiently transfected with FLAG-tagged HIF-1α plasmid or empty vector (p3 × FLAG-CMV) and exposed to IH_{60} or normoxia and treated with vehicle or CTK7A (25 μM). TBP is shown as a loading control run on the same gel. (*D*) HIF-1α was immunoprecipitated with anti-FLAG antibody from nuclear extracts (600 μg) of cells transiently transfected with FLAG-tagged HIF-1α overexpression plasmids and exposed to IH_{60} or normoxia with or without CTK7A (25 μM) treatment. HIF-1α protein, HIF-1α acetylation, and p300/CBP protein levels were analyzed in replicates of the immunoprecipitates run on the same gel and probed using anti-HIF1α, anti-acetylated lysine, and p300/CBP antibodies, respectively, by immunoblots. (*E*) Densitometric analysis of the immune blots showing ratio of acetyl HIF-1α to total HIF-1α. (*F*) Densitometric analysis of the immune blots showing p300/CBP coimmunoprecipitated with HIF-1α. *P* values (**$P \leq 0.01$ and *$P < 0.05$) between different groups as determined by *post hoc* Tukey HSD test. Data are mean ± SEM from three experiments. IP = immunoprecipitate.

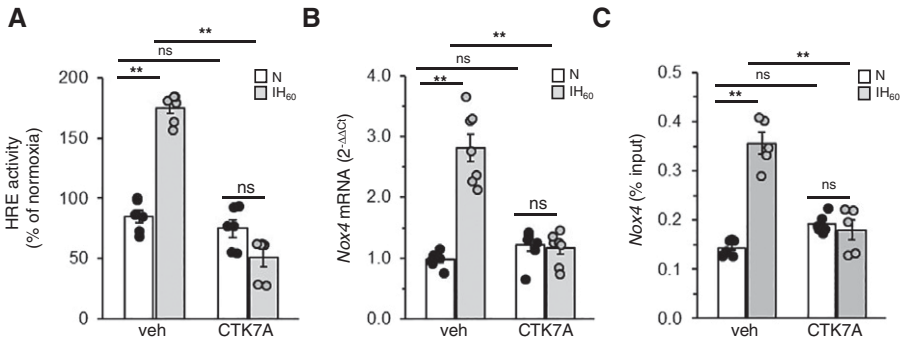

Figure 4. P300/CBP contributes to HIF-1–mediated transcription by IH. (*A*) Hypoxia response element (HRE) transcriptional activity in nuclear lysates of cells transfected with a plasmid p2.1, containing HRE upstream of SV40 promoter and luciferase coding sequence, and the *Renilla* luciferase control vector exposed to IH_{60} or normoxia with or without CTK7A (25 μM). (*B*) *Nox4* mRNA in PC12 cells exposed to IH_{60} or normoxia treated with CTK7A. (*C*) *Nox4* enrichment in the immunoprecipitates from PC12 cells treated with CTK7A and exposed to IH_{60} or normoxia as determined by chromatin immunoprecipitation (ChIP) assay using antibodies against HIF-1α. Data are represented as percentage of input (mean ± SEM) from five to seven independent experiments. *P* values (**$P \leq 0.01$) between different groups as determined by *post hoc* Tukey HSD test.

P300/CBP Participates in HIF-1 Transcriptional Activation by IH

The role of p300/CBP in HIF-1 transcriptional activity by IH was determined by transfecting cells with a plasmid containing an HRE upstream of luciferase coding sequences. Cells were then exposed to IH or room air (controls), with or without CTK7A. IH led to robust activation of HIF-1 transcription, as evidenced by increased luciferase activity, and this effect was absent in CTK7A-treated cells (Figure 4A).

HIF-1 transcriptional activity is driven by HIF-1α binding to the HRE in the promoter regions of target genes (29, 30). We and others have shown binding of HIF-1α to the HRE of the promoter region of the *Nox4* gene (24, 31). Therefore, we determined the effect of IH on *Nox4* mRNA. IH increased *Nox4* mRNA, and CTK7A blocked this effect (Figure 4B). Further analysis by chromatin immunoprecipitation (ChIP) assay showed the absence of HIF-1α binding to the HRE site in the promoter region of the *Nox4* gene in CTK7A-treated cells exposed to IH compared with untreated cells (Figure 4C). These data demonstrate interaction of p300/CBP with HIF-1α is necessary for binding of HIF-1 to the HRE site of the *Nox4* gene.

P300/CBP Contribution to HIFI-Signaling in IH-treated Rats

Thus far, studies on cell cultures suggest that p300/CBP regulates HIF-1–dependent transcriptional activation by IH. We next sought to validate the role of p300/CBP in HIF-1 transcription in rats treated with IH. We studied male rats to exclude behavioral variations arising from the estrous cycle in female rats.

Rats were treated with IH for 10 days, and KAT activity as well as p300/CBP and HIF-1α protein levels were analyzed in the AM. AM tissue was chosen because: *1*) PC12 cells studied in the cell culture experiments are of adrenal medullary chromaffin cell origin (20); and *2*) the AM is critical for evoking IH-induced hypertension (32). KAT enzyme activity, p300/CBP, and HIF-1α protein were increased in the AM of IH-treated rats (Figures 5A–5C). These effects were absent in IH-exposed rats treated with CTK7A (2 mg/kg intraperitoneally every day for 10 d) (Figures 5A–5C).

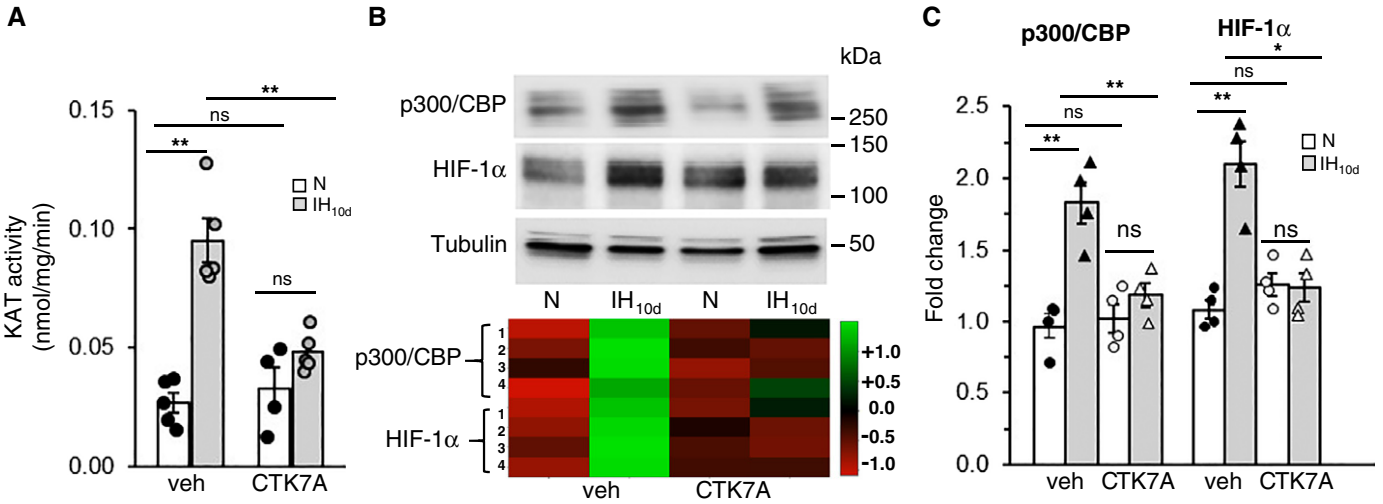

Figure 5. P300/CBP activation increases HIF-1α in the adrenal medulla (AM) of IH-exposed rats. Rats exposed to room air or 10 days of IH (IH_{10d}) were treated daily with either vehicle or CTK7A (2 mg/kg/d, intraperitoneal). (*A*) Effect of CTK7A treatment on KAT activity. (*B*) Top panel: representative immunoblot showing p300/CBP and HIF-1α protein expression. Tubulin is shown as loading control run on the same gel. Bottom panel: data shown as heat map generated from raw pixel data for each protein normalized to loading control (tubulin) and scaled using R studio (v4.2.2) and heatmaply (43). Numbers denote the number of experiments. (*C*) Densitometric analysis of the immunoblots showing fold change in expression of p300/CBP and HIF-1α relative to a vehicle-treated normoxia control. *P* values (**$P \leq 0.01$ and *$P < 0.05$) between different groups as determined by *post hoc* Tukey HSD test. Data presented as mean ± SEM and individual data points from 8 to 10 rats per group.

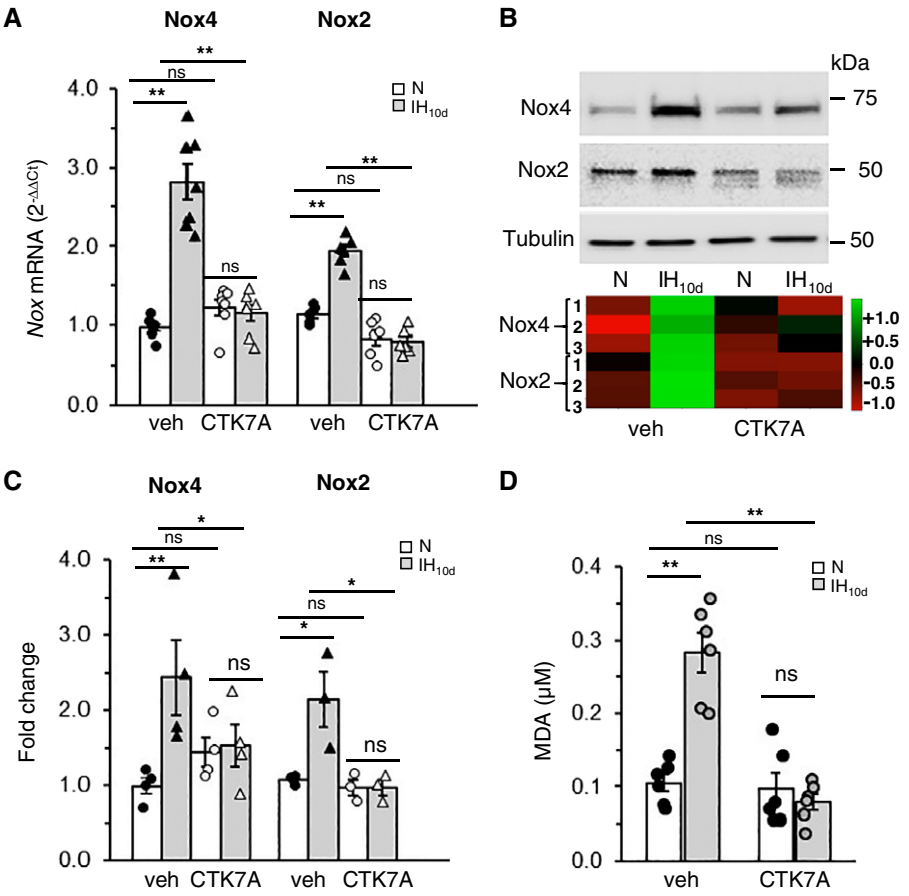

Figure 6. P300/CBP activation contributes to *NADPH oxidase* gene expression and reactive oxygen species (ROS) generation in the AM of rats exposed to IH. (*A*) Effect of CTK7A on *Nox4* and *Nox2* mRNA. (*B*) Top panel: immunoblots showing replicates of total lysates run on separate gel and analyzed for Nox4 and Nox2 protein expression with tubulin as loading control. Bottom panel: heat map. (*C*) Densitometric analysis of the immunoblots showing fold change in Nox4 and Nox2 relative to a vehicle-treated normoxic control. (*D*) MDA measured as in index of ROS in cell lysates of AM. *P* values (**$P \leq 0.01$ and *$P < 0.05$) between different groups as determined by *post hoc* Tukey HSD test. Data shown are mean ± SEM together with individual data points from eight rats per group. MDA = malondialdehyde.

Lower doses of CTK7A (0.5 or 1 mg/kg intraperitoneally) were ineffective in inhibiting KAT activity. These results were essentially the same as that seen in IH-treated PC12 cells and suggest a role for p300/CBP in HIF-1α increase by IH in rat AM.

To assess the functional significance of p300/CBP-dependent stabilization of HIF-1α in IH-treated rats, mRNAs encoding *Nox2* and *Nox4* and the corresponding protein abundances were determined. IH-exposed rats showed elevated *Nox4* and *Nox2* mRNA expression (Figure 6A) as well as corresponding proteins (Figure 6B), and these responses were either reduced or blocked by CTK7A treatment (Figures 6A–6C). *NADPH* oxidase activation increases reactive oxygen species (ROS). MDA concentrations representing oxidized lipids were measured as an index of ROS generation. IH increased MDA amounts in the AM of vehicle-treated rats, which was absent in CTK7A-treated rats (Figure 6D). These findings suggest participation of p300/CBP in HIF-1–mediated transcription of the *Nox2* and *Nox4* genes by IH.

P300/CBP Contributes to Heightened Sympathetic Activity and Hypertension by IH

ROS signaling arising from HIF-1–dependent transcription of prooxidant enzymes (Nox) contributes to sympathetic nerve activation and hypertension in IH-treated rats (9). We hypothesized that blockade of HIF-1 transcription by inhibiting p300/CBP with CTK7A should prevent IH-induced sympathetic nerve activation and hypertension. This possibility was assessed by measuring plasma norepinephrine concentration as an index of activation of the sympathetic nervous system and BP in IH-exposed rats with and without CTK7A treatment. IH increased systolic, diastolic, and mean BP in rats exposed to 10 days of IH compared with control rats treated with room air, and these effects were absent in CTK7A-treated rats exposed to IH (Figures 7A–7C). Likewise, the plasma NE amounts elevated in IH-exposed rats decreased significantly with CTK7A treatment (Figure 7D).

Discussion

Our cell culture studies showed that: *1*) IH increased KAT activity by selectively increasing p300/CBP protein; *2*) IH increased autoacetylation of p300/CBP acetylates and stabilized HIF-1α protein; and *3*) increased HIF-1 transcription requires binding of p300/CBP to HIF-1α. IH-treated

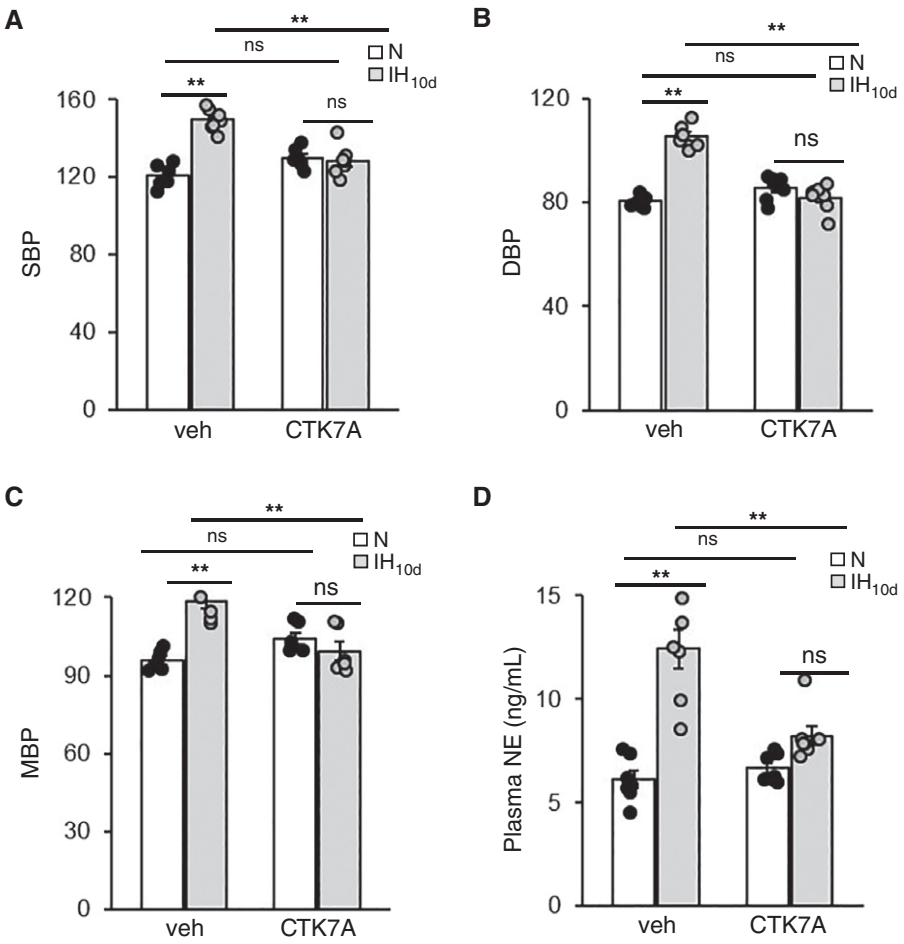

Figure 7. CTK7A (p300/CBP inhibitor) blocks elevated blood pressure and plasma norepinephrine (NE) changes in IH-exposed rats. (*A–C*) SBP, DBP, and MBP and (*D*) plasma NE levels in IH- or normoxia-exposed rats treated with vehicle or CTK7A. Data shown are mean ± SEM together with individual points from eight rats per group. *P* values (**$P \leq 0.01$) between different groups as determined by *post hoc* Turkey HSD test. DBP = diastolic blood pressure; MBP = mean blood pressure; SBP = systolic blood pressure.

rats also showed increased p300/CBP protein in AM tissue, and this effect was associated with elevated plasma catecholamine concentrations and BP. IH-evoked sympathetic nerve activation and hypertension were absent in IH-exposed rats with pharmacological inhibition of p300/CBP with CTK7A.

The following findings demonstrate that p300/CBP are the major KAT enzymes responsible for the increased KAT enzyme activity. *1*) IH selectively increased p300/CBP protein expression, whereas PCAF and GCN5 were decreased; and *2*) pharmacological blockade of p300/CBP with CTK7A inhibited IH-evoked increase of KAT activity and p300/CBP protein. CTK7A affected baseline KAT activity in PC12 cells, which was not observed in the AM of rats. The differences between *in vivo* and *in vitro* experiments are likely due to differences in the dose of CTK7A and/or duration of IH, wherein cell cultures were exposed to several hours of IH as opposed to 10-day exposure in rats. The relatively longer duration of IH exposure in rats might have led to compensatory mechanisms. We could not delineate individual roles of p300 and CBP because: *1*) the antibodies used in this study recognize both p300 and CBP; *2*) there was a lack of specific inhibitors for p300 versus CBP; and *3*) genetic silencing of p300 or CBP by siRNA approach impaired cell viability under normoxic conditions, which was worsened with IH.

How might IH increase p300/CBP protein? Post-translational modifications affect p300/CBP protein stability positively or negatively, depending on the site (33). Acetylation of p300/CBP is a well-studied post-translational modification. Reversible autoacetylation of the regulatory loop of p300/CBP stabilizes, stimulates its acetyl transferase activity, and increases its binding affinity (28, 33, 34). IH increased total p300/CBP and acetylated p300/CBP protein (Figure 2D), and these effects are blocked by CTK7A, suggesting that IH-increased p300/CBP protein expression is attributable to its lysine acetylation status. These findings are reminiscent of a recent report showing that CTK7A also inhibits p300-autoacetylation in gastric cancer cell lines (17). P300/CBP can also be phosphorylated at several sites by kinases, including PKC, cyclin E/CDK-2, CaMK IV, ERK2, and AKT (35). An earlier study from our laboratory showed increased phosphorylation of p300/CBP by CamK II increases HIF-1–mediated transactivation, suggesting that post-translational modifications involving phosphorylation also play a role in IH-increased p300/CBP protein expression

(14). It remains to be established whether crosstalk between p300/CBP acetylation and phosphorylation lead to greater expression of p300/CBP under the setting of IH. HIF-1α is known to be acetylated at multiple sites by different KATs, with different biological consequences. For instance, PCAF is primarily responsible for Lys^{674} acetylation (36), whereas p300 acetylates Lys^{709} in HIF-1α (19). Although IH increased HIF-1α acetylation, our study did not attempt to identify specific lysine residue acetylated by IH. Notwithstanding this limitation, we found CTK7A blocked HIF-1α acetylation and HIF-1α protein elevation by IH. These findings suggest that lysine acetylation by p300/CBP contributes to HIF-1α stabilization by IH.

P300/CBP can bind to different transcription factors by directly interacting with various proteins and/or serve as a scaffold to bring a complex of diverse cofactor proteins to the promoters on chromatin allowing transcriptional activation (33). The finding that HIF-1α coimmunoprecipitated with p300/CBP in IH-treated cells demonstrates physical binding of p300/CBP to HIF-1α. CTK7A not only blocked p300/CBP protein stability but also inhibited p300/CBP binding to HIF-1α and HIF-1 binding to the HRE on the *Nox4* gene. Together, these findings suggest that p300/CBP exists in a stable complex with HIF-1α and facilitates activation of HIF-1–dependent *Nox4* transcription by IH. Dehydroxylation at asparagine^{803} increases HIF-1α–p300 interaction, shifting Lys^{709} to an acetylated state, thereby contributing to HIF-1α protein stability and HIF-1 transactivation (37). Additional studies are needed to assess whether p300/CBP interaction with HIF-1α is dependent on aspargine^{803} hydroxylation and whether lys^{709} in particular is acetylated by p300/CBP under IH conditions.

Emerging evidence suggests that IH is a major contributor to hypertension, a common comorbidity associated with OSA (6). Previous studies have shown HIF-1–dependent transcriptional activation of the prooxidant *Nox* genes, and the ensuing ROS signaling is a major cellular mechanism underlying IH-induced sympathetic nerve activation and the resulting hypertension (6). The current study showed systemic administration of the p300/CBP inhibitor CTK7A prevented HIF-1α stabilization, *Nox4* upregulation, activation of the sympathetic nervous system as indicated by absence of elevated plasma NE concentration, and hypertension in IH-exposed rats. These findings provide evidence for the hitherto unexplored role of p300/CBP in autonomic dysregulation by IH as it relates to OSA.

Interactions of p300/CBP with transcription factors are involved in the development of a variety of diseases (33, 38, 39) comprising viral infections, cognitive disorders, Alzheimer's disease, diabetes, and cardiovascular diseases. Acetylation and the protein binding function of P300/CBP are intricately interrelated, and both sites are targets for the treatment of cancer (40) and many other diseases (41, 42). Our study of a rodent model of sleep apnea with IH suggest that pharmacological targeting of p300/CBP acetylation with CTK7A might be a novel therapeutic alternative for preventing cardiovascular morbidity. ■

Author disclosures are available with the text of this article at www.atsjournals.org.

References

1. Nieto FJ, Young TB, Lind BK, Shahar E, Samet JM, Redline S, *et al.* Association of sleep-disordered breathing, sleep apnea, and hypertension in a large community-based study: Sleep Heart Health Study. *JAMA* 2000;283:1829–1836.
2. Young T, Finn L, Peppard PE, Szklo-Coxe M, Austin D, Nieto FJ, *et al.* Sleep disordered breathing and mortality: eighteen-year follow-up of the Wisconsin sleep cohort. *Sleep* 2008;31:1071–1078.
3. Bao G, Metreveli N, Li R, Taylor A, Fletcher EC. Blood pressure response to chronic episodic hypoxia: role of the sympathetic nervous system. *J Appl Physiol (1985)* 1997;83:95–101.
4. Prabhakar NR, Peng YJ, Kumar GK, Nanduri J. Peripheral chemoreception and arterial pressure responses to intermittent hypoxia. *Compr Physiol* 2015;5:561–577.
5. Fletcher EC, Bao G. The rat as a model of chronic recurrent episodic hypoxia and effect upon systemic blood pressure. *Sleep* 1996;19: S210–S212.
6. Prabhakar NR, Peng YJ, Nanduri J. Hypoxia-inducible factors and obstructive sleep apnea. *J Clin Invest* 2020;130:5042–5051.
7. Yuan G, Nanduri J, Khan S, Semenza GL, Prabhakar NR. Induction of HIF-1alpha expression by intermittent hypoxia: involvement of NADPH oxidase, Ca2+ signaling, prolyl hydroxylases, and mTOR. *J Cell Physiol* 2008;217:674–685.
8. Semenza GL, Prabhakar NR. HIF-1-dependent respiratory, cardiovascular, and redox responses to chronic intermittent hypoxia. *Antioxid Redox Signal* 2007;9:1391–1396.
9. Peng YJ, Yuan G, Ramakrishnan D, Sharma SD, Bosch-Marce M, Kumar GK, *et al.* Heterozygous HIF-1alpha deficiency impairs carotid body-mediated systemic responses and reactive oxygen species generation in mice exposed to intermittent hypoxia. *J Physiol* 2006;577:705–716.
10. Brahimi-Horn C, Mazure N, Pouysségur J. Signalling via the hypoxia-inducible factor-1alpha requires multiple posttranslational modifications. *Cell Signal* 2005;17:1–9.
11. Daly LA, Brownridge PJ, Batie M, Rocha S, Sée V, Eyers CE. Oxygen-dependent changes in binding partners and post-translational modifications regulate the abundance and activity of HIF-1α/2α. *Sci Signal* 2021;14:eabf6685.
12. Yao TP, Oh SP, Fuchs M, Zhou ND, Ch'ng LE, Newsome D, *et al.* Gene dosage-dependent embryonic development and proliferation defects in mice lacking the transcriptional integrator p300. *Cell* 1998;93: 361–372.
13. Tanaka Y, Naruse I, Hongo T, Xu M, Nakahata T, Maekawa T, *et al.* Extensive brain hemorrhage and embryonic lethality in a mouse null mutant of CREB-binding protein. *Mech Dev* 2000;95: 133–145.
14. Yuan G, Nanduri J, Bhasker CR, Semenza GL, Prabhakar NR. Ca2+/ calmodulin kinase-dependent activation of hypoxia inducible factor 1 transcriptional activity in cells subjected to intermittent hypoxia. *J Biol Chem* 2005;280:4321–4328.
15. Arany Z, Huang LE, Eckner R, Bhattacharya S, Jiang C, Goldberg MA, *et al.* An essential role for p300/CBP in the cellular response to hypoxia. *Proc Natl Acad Sci USA* 1996;93:12969–12973.
16. Kasper LH, Boussouar F, Boyd K, Xu W, Biesen M, Rehg J, *et al.* Two transactivation mechanisms cooperate for the bulk of HIF-1-responsive gene expression. *EMBO J* 2005;24:3846–3858.
17. Rath S, Jena AB, Bhattacharyya A, Dandapat J. CTK7A, a curcumin derivative, can be a potential candidate for targeting HIF-1α/p300 complex: evidences from in vitro and computational studies. *Biophys Chem* 2022;287:106828.
18. Dengler VL, Galbraith M, Espinosa JM. Transcriptional regulation by hypoxia inducible factors. *Crit Rev Biochem Mol Biol* 2014;49:1–15.
19. Geng H, Liu Q, Xue C, David LL, Beer TM, Thomas GV, *et al.* HIF1α protein stability is increased by acetylation at lysine 709. *J Biol Chem* 2012;287:35496–35505.
20. Greene LA, Tischler AS. Establishment of a noradrenergic clonal line of rat adrenal pheochromocytoma cells which respond to nerve growth factor. *Proc Natl Acad Sci USA* 1976;73:2424–2428.

21. Yuan G, Adhikary G, McCormick AA, Holcroft JJ, Kumar GK, Prabhakar NR. Role of oxidative stress in intermittent hypoxia-induced immediate early gene activation in rat PC12 cells. *J Physiol* 2004;557:773–783.
22. Nanduri J, Wang N, Yuan G, Khan SA, Souvannakitti D, Peng YJ, *et al.* Intermittent hypoxia degrades HIF-2alpha via calpains resulting in oxidative stress: implications for recurrent apnea-induced morbidities. *Proc Natl Acad Sci USA* 2009;106:1199–1204.
23. Semenza GL, Jiang BH, Leung SW, Passantino R, Concordet JP, Maire P, *et al.* Hypoxia response elements in the aldolase A, enolase 1, and lactate dehydrogenase A gene promoters contain essential binding sites for hypoxia-inducible factor 1. *J Biol Chem* 1996;271: 32529–32537.
24. Nanduri J, Wang N, Wang BL, Prabhakar NR. Lysine demethylase KDM6B regulates HIF-1α-mediated systemic and cellular responses to intermittent hypoxia. *Physiol Genomics* 2021;53:385–394.
25. Finnin MS, Donigian JR, Cohen A, Richon VM, Rifkind RA, Marks PA, *et al.* Structures of a histone deacetylase homologue bound to the TSA and SAHA inhibitors. *Nature* 1999;401:188–193.
26. Bertrand P. Inside HDAC with HDAC inhibitors. *Eur J Med Chem* 2010; 45:2095–2116.
27. Arif M, Vedamurthy BM, Choudhari R, Ostwal YB, Mantelingu K, Kodaganur GS, *et al.* Nitric oxide-mediated histone hyperacetylation in oral cancer: target for a water-soluble HAT inhibitor, CTK7A. *Chem Biol* 2010;17:903–913.
28. Jain S, Wei J, Mitrani LR, Bishopric NH. Auto-acetylation stabilizes p300 in cardiac myocytes during acute oxidative stress, promoting STAT3 accumulation and cell survival. *Breast Cancer Res Treat* 2012;135: 103–114.
29. Wang GL, Semenza GL. Characterization of hypoxia-inducible factor 1 and regulation of DNA binding activity by hypoxia. *J Biol Chem* 1993; 268:21513–21518.
30. Wenger RH, Stiehl DP, Camenisch G. Integration of oxygen signaling at the consensus HRE. *Sci STKE* 2005;2005:re12.
31. Diebold I, Petry A, Hess J, Görlach A. The NADPH oxidase subunit NOX4 is a new target gene of the hypoxia-inducible factor-1. *Mol Biol Cell* 2010;21:2087–2096.
32. Prabhakar NR, Kumar GK, Peng YJ. Sympatho-adrenal activation by chronic intermittent hypoxia. *J Appl Physiol (1985)* 2012;113:1304–1310.
33. Dancy BM, Cole PA. Protein lysine acetylation by p300/CBP. *Chem Rev* 2015;115:2419–2452.
34. Karanam B, Jiang L, Wang L, Kelleher NL, Cole PA. Kinetic and mass spectrometric analysis of p300 histone acetyltransferase domain autoacetylation. *J Biol Chem* 2006;281:40292–40301.
35. Chan HM, La Thangue NB. p300/CBP proteins: HATs for transcriptional bridges and scaffolds. *J Cell Sci* 2001;114:2363–2373.
36. Lim JH, Lee YM, Chun YS, Chen J, Kim JE, Park JW. Sirtuin 1 modulates cellular responses to hypoxia by deacetylating hypoxia-inducible factor 1alpha. *Mol Cell* 2010;38:864–878.
37. Luo W, Wang Y. Epigenetic regulators: multifunctional proteins modulating hypoxia-inducible factor-α protein stability and activity. *Cell Mol Life Sci* 2018;75:1043–1056.
38. Zhang L, Sheng C, Zhou F, Zhu K, Wang S, Liu Q, *et al.* CBP/p300 HAT maintains the gene network critical for β cell identity and functional maturity. *Cell Death Dis* 2021;12:476.
39. Valor LM, Viosca J, Lopez-Atalaya JP, Barco A. Lysine acetyltransferases CBP and p300 as therapeutic targets in cognitive and neurodegenerative disorders. *Curr Pharm Des* 2013;19:5051–5064.
40. Cheng Y, He C, Wang M, Ma X, Mo F, Yang S, *et al.* Targeting epigenetic regulators for cancer therapy: mechanisms and advances in clinical trials. *Signal Transduct Target Ther* 2019;4:62.
41. Brown JA. Patent spotlight: small-molecule lysine acetyltransferase inhibitors (KATi). *Pharm Pat Anal* 2020;9:17–28.
42. Wapenaar H, Dekker FJ. Histone acetyltransferases: challenges in targeting bi-substrate enzymes. *Clin Epigenetics* 2016;8:59.
43. Galili T, O'Callaghan A, Sidi J, Sievert C. heatmaply: an R package for creating interactive cluster heatmaps for online publishing. *Bioinformatics* 2018;34:1600–1602.